∇ = vector differential operator

Subscripts

A, B = components A, B, etc.
AB = binary system composed of components A and B
avg = average value of a quantity
0 = evaluated at the interfacial position
∞ = quantity evaluated at a large distance from the gas-liquid interface, equivalent to inlet conditions

LITERATURE CITED

1. Arnold, J. H., *Trans. AIChE*, **40**, 361 (1944).
2. Bird, R. B., W. E. Stewart, and E. N. Lightfoot, "Transport Phenomena," John Wiley, New York (1960).
3. Byers, C. H., and C. J. King, *AIChE J.*, **13**, 628 (1967).
4. *Ibid.*, **13**, 637 (1967).
5. Cairns, R. C., and G. H. Roper, *Chem. Eng. Sci.*, **3**, 97 (1954).
6. Carslaw, H. S., and J. C. Jaeger, "Conduction of Heat in Solids," Oxford University Press, 2nd Ed., New York (1959).
7. Clark, M. W., and C. J. King, *U.S. Atomic Energy Comm.*, Rept. UCRL 17527 (1967).
8. Colburn, A. P., and T. B. Drew, *Trans. AIChE*, **33**, 197 (1937).
9. Emanuel, A. S., and D. R. Olander, *Intern. J. Heat Mass Transfer*, **7**, 539 (1964).
10. Lapidus, L., "Digital Computation for Chemical Engineers," McGraw-Hill, New York (1962).
11. Lewis, W. K., and C. K. Chang, *Trans. AIChE*, **21**, 127 (1928).
12. Lightfoot, E. N., and E. L. Cussler, Jr., *Chem. Eng. Progr. Symp. Ser.*, **61**, No. 58, 66 (1965).
13. Mendelson, H., and A. Yerazunis, *AIChE J.*, **11**, 834 (1965).
14. Modine, A. D., E. B. Parrish, and H. L. Toor, *ibid.*, **9**, 348 (1963).
15. Olander, D. R., *J. Phys. Chem.*, **67**, 1011 (1963).
16. Ranz, W. E., and P. F. Dickson, *Ind. Eng. Chem. Fundamentals*, **4**, 345 (1965).
17. Shulman, H. L., and L. J. Delaney, *AIChE J.*, **5**, 290 (1959).
18. Vivian, J. E., and W. C. Behrmann, *ibid.*, **11**, 656 (1965).
19. Wasan, D. T., and C. R. Wilke, *U.S. Atomic Energy Comm.*, Rept. UCRL-11629 (1964).
20. Westkaemper, L. E., and R. R. White, *AIChE J.*, **3**, 69 (1957).
21. Wilke, C. R., and C. Y. Lee, *Ind. Eng. Chem.*, **47**, 1253 (1955).

Part II. Liquid Mixtures

An approach has been developed for predicting rates of interphase mass transfer under conditions of high flux and high concentration level. A rectangular channel device has been used to measure rates of evaporation of four solutes, carbon disulfide, *n*-pentane, cyclopentane, and ethyl ether, from *n*-tridecane into flowing nitrogen. The evaporation rate of carbon disulfide agreed with the prediction of the interphase theory up to a carbon disulfide mole fraction of 0.30 in the bulk liquid. For the other three systems, a concentration gradient induced, surface tension driven cellular convection served to increase liquid-phase coefficients substantially. A correlation was obtained for the effect of this cellular motion on the liquid-phase mass transfer coefficient.

In part I of this series, the prediction of evaporation rates was simplified by the lack of liquid-phase mass transfer resistance. The calculation of mass transfer rates for the evaporation of liquid mixtures is considerably more complex, since the mass transfer resistance can lie in both the gas and liquid phases. The interfacial gas-phase composition is a function of interfacial temperature and the ratio of the mass transfer coefficients in the two phases. The problem requires the simultaneous solution of the convective transport equations for both phases. If the complicating factors of high flux and high concentration level are also important, the problem becomes still more difficult.

The experimental equipment utilized in this study was the same rectangular duct described in part I. A number of different volatile compounds were vaporized from a flowing nonvolatile solvent (*n*-tridecane) into a flowing nitrogen stream. The mass transfer conditions could be varied by changing either the nature or the concentration of the evaporating substance, or the temperature. Since the equipment has already demonstrated predictable behavior with respect to the stream flow variables (7 to 9), the flow conditions were fixed for all runs. The inlet nitrogen flow rate was held at 166 cc./sec., while the feed liquid flow was 0.400 gal./min. The interfacial temperature was controlled to within 0.2°C. of a constant value for each solute system.

INTERPHASE MASS TRANSFER

The first major contributions toward the solution of the general two-phase resistance, mass transfer problem were made by Lewis (*16*) and Whitman (27). Their approach resulted in a simple addition of independently measured individual phase resistances to yield the overall mass transfer resistance. There are a number of criteria which must be satisfied in order for the additivity of independently measured individual phase resistances to be valid (*12*). The effects of deviations from these criteria tend to cancel out one another in simple equipment providing only a single exposure of the contacting phases, particularly when the additivity principle is applied to the average rather than the local mass transfer coefficients. In complex contacting equipment, such as packed and plate columns, the departure from additivity can be much more severe.

For concurrent flow in the device used in this study, the additivity of resistances principle is accurate to better than 2% for low flux and low concentration levels, provided the the Graetz number ($D_{AB}L/U_{avg}b^2$) is less than 0.50 (*8, 9*). Independently measured resistances tend to be additive if the individual coefficients have similar functionalities with respect to exposure time, or length of contact between phases. Since the high flux and high concentration level corrections do not affect the x direction functionality of the individual phase mass transfer coefficients, the additivity principle should work as well under conditions of high flux and high concentration level, provided the correction factors for these effects are properly applied.

A convenient and accurate assumption for most liquid-phase mass transfer calculations is that of constant partial molal volume, which leads to a liquid-phase mass transfer coefficient based on volume fraction driving forces:

$$\dot{k}_{\phi,\,\mathrm{loc}} = \frac{N_{A0} - \varphi_{A0}[N_{A0} + (\tilde{V}_B/\tilde{V}_A)N_{B0}]}{\varphi_{A0} - \varphi_{A\infty}} \quad (1)$$

By analogy to the procedure followed in part I for the gas phase

$$k_{\phi,\,\mathrm{loc}} = \lim [\dot{k}_{\phi,\,\mathrm{loc}}]$$

$$[N_{A0} + (\tilde{V}_B/\tilde{V}_A)N_{B0}] \to 0 \quad (2)$$

$$R_{AB,\,L} = \frac{\varphi_{A0} - \varphi_{A\infty}}{\dfrac{N_{A0}}{N_{A0} + (\tilde{V}_B/\tilde{V}_A)N_{B0}} - \varphi_{A0}} \quad (3)$$

$$\theta_{AB,\,L} = \dot{k}_{\phi}/k_{\phi} \quad (4)$$

It is also convenient to define average mass transfer coefficients, for example

$$\dot{k}_{\phi,\,\mathrm{avg}} = \frac{N_{A0(\mathrm{avg})} - \varphi_{A0(\mathrm{avg})}[N_{A0(\mathrm{avg})} + (V_B/V_A)N_{B0(\mathrm{avg})}]}{\varphi_{A0(\mathrm{avg})} - \varphi_{A\infty}} \quad (5)$$

where the interfacial flux and concentration variables are averaged over the entire mass transfer exposure.

If we now assume that $N_{B0} = 0$ and divide Equation (5) into its gas-phase equivalent, while realizing that $-N_{A0,\,G}$ must be equal to $N_{A0,\,L}$, we obtain

$$\frac{\dot{k}_{x,\,\mathrm{avg}}}{\dot{k}_{\phi,\,\mathrm{avg}}} = -\frac{(\varphi_{A0} - \varphi_{A\infty})(1 - x_{A0})}{(x_{A0} - x_{A\infty})(1 - \varphi_{A0})} = \frac{k_{x,\,\mathrm{avg}}\,\theta_{AB,\,G}}{k_{\phi,\,\mathrm{avg}}\,\theta_{AB,\,L}} \quad (6)$$

If we presume that

$$p_A = x_A P \quad (7)$$

assume constant partial molal volumes and adopt a linear equilibrium expression

$$p_A = HC_{AL} + \text{constant} \quad (8)$$

ϕ_{A0} and x_{A0} may be related by

$$x_{A0} = (H/p\tilde{V}_A)\,\varphi_{A0} + (\text{constant}) \quad (9)$$

Equations (6) and (9) determine the two unknown interfacial concentrations x_{A0} and ϕ_{A0}. Equation (6) is implicit because $\theta_{AB,\,G}$ and $\theta_{AB,\,L}$ are dependent upon the interfacial concentrations. An iterative procedure was employed to achieve the solution, as follows:

1. Use the low flux, low concentration level solutions for each phase separately to obtain trial values of x_{A0} and φ_{A0} from Equations (6) and (9). Ignore the θ_{AB}, $1 - x_{A0}$, and $1 - \varphi_{A0}$ factors.

2. Using these values for x_{A0} and φ_{A0}, obtain a value of $R_{AB,\,L}$ from Equation (3) and a value of $R_{AB,\,G}$ from the analogous gas-phase expression. Use the penetration or Leveque curve (Figure 1, part I) to obtain values for $\theta_{AB,\,L}$ and $\theta_{AB,\,G}$.

3. Solve Equations (6) and (9) for new values of x_{A0} and ϕ_{A0} using these values of $\theta_{AB,\,L}$ and $\theta_{AB,\,G}$. Return to Step 2 and repeat the calculation until convergence is achieved.

The average flux was then calculated from Equation (5) and was converted into the fraction saturation of the gas phase (F_s), defined as the ratio of the cup-mixing gas-phase solute mole fraction to the mole fraction which would be in equilibrium with the bulk liquid composition at the interfacial temperature.

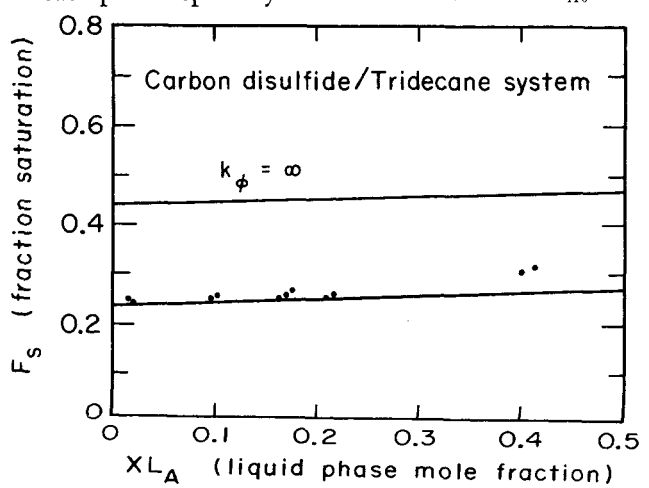

Fig. 1. Evaporation of carbon disulfide from *n*-tridecane.

PHYSICAL PROPERTIES

Four different binary liquid systems were used during the course of the experiments. In each case the nonvolatile solvent was *n*-tridecane. The volatile species were *n*-pentane, cyclopentane, ethyl ether, and carbon disulfide. For each of these systems it was necessary to obtain several physical properties for use in the equations to predict F_s from theory. Values of these physical properties are summarized in Table 1.

Vapor-liquid equilibrium data were measured experimentally for each system as a function of concentration level by determining the bulk exit gas composition for a number of runs made at very low gas flow rates. These data are reported in detail elsewhere (*10*) and were used as the basis for computing F_s. It was found that all systems agreed reasonably well with Raoult's law; the most extreme deviations occurred for ethyl ether, which exhibited an activity coefficient of about 1.25 at high dilution in *n*-tridecane.

Surface tensions were taken from standard references (*1, 24*); those for *n*-tridecane were calculated to be 26.1

Table 1. Physical Properties for Different Solutes

	n-pentane	Cyclo pentane	Ethyl ether	Carbon disulfide
T_0, °C.	20	25	25	30
vapor pressure at T_0, mm. Hg	418.8	314.9	535.1	426.4
surface tention, dyne/cm.				
20°C.	16.00	22.57	17.06	33.07
30°C.	—	21.17	15.95	32.25
density, g./ml.				
20°C.	0.626	0.745	0.714	1.263
30°C.	0.616	0.735	0.702	1.250
gas-phase diffusivity with N_2 at T_0, sq. cm./sec.	0.0882	0.0943	0.0975	0.1112
viscosity constants at T_0 for mixtures with *n*-tridecane				
A	1.92	1.730	1.730	1.565
B	−2.74	−1.323	−2.332	−1.220
C	1.06	0	0.824	0
diffusivities at T_0 at high dilution, sq. cm./sec. × 10^5				
a. solute in *n*-tridecane	1.10	1.16	1.17	1.33
b. *n*-tridecane in solute	3.71	1.97	3.82	2.88

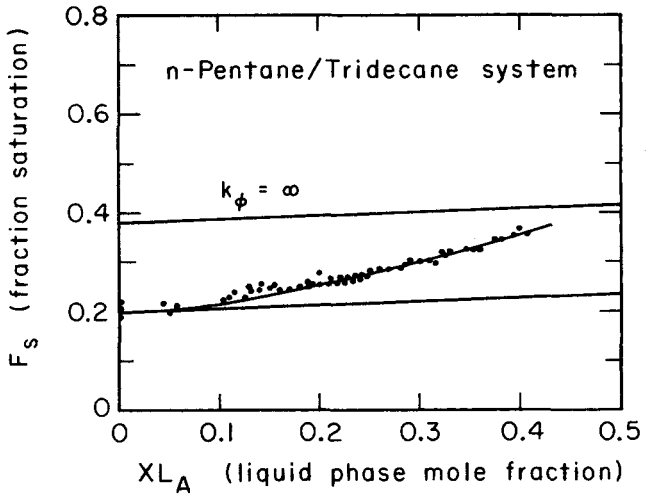

Fig. 2. Evaporation of *n*-pentane from *n*-tridecane. $T_0 = 20°C$.

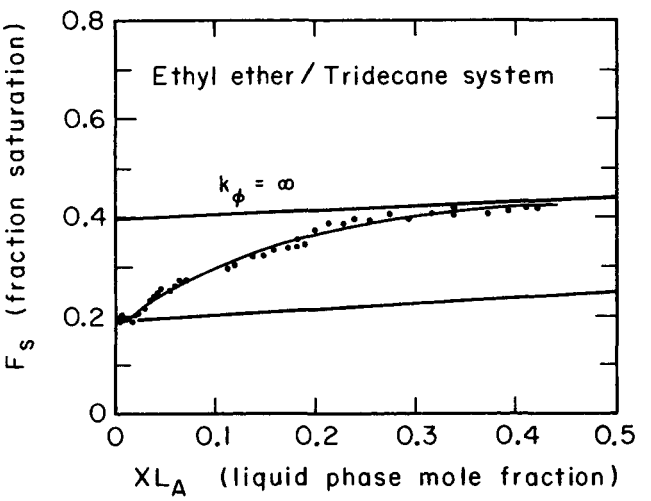

Fig. 4. Evaporation of ethyl ether from *n*-tridecane. $T_0 = 25°C$.

and 25.2 dynes/cm. at 20° and 30°C., respectively. Surface tensions of liquid mixtures were computed as

$$\gamma_{mix} = \sum_j x_j \gamma_j \qquad (10)$$

Koefoed and Villadsen (*14*) report surface tensions for heptane-hexadecane mixtures as a function of composition. From their data it can be concluded that values of $(\partial\gamma/\partial x_A)$ computed from Equation (*10*) will be within 5 to 15% of the true value for the various experimental situations encountered in this study.

Densities were determined with a 10 ml. pycnometer. The density of *n*-tridecane was found to be 0.756 and 0.749 g./ml. at 20° and 30°C., respectively. Densities for all liquid mixtures showed that there was essentially no volume change upon mixing, thus validating the assumption of constant $\tilde{V}_A$ and $\tilde{V}_B$.

Gas-phase diffusivities were computed by the methods reported in part I of this series.

Liquid viscosities were measured as a function of composition with a capillary flow viscometer, kept isothermal in a constant temperature bath. The results were fitted to a polynomial of the form

$$\mu(cp) = A + B\,(XL_A) + C\,(XL_A)^2 \qquad (11)$$

Values of the constants are given in Table 1.

Liquid-phase diffusivities were obtained as a function of concentration by taking the group $D_{AB}\mu$ to be linear in mole fraction. Bidlack and Anderson (*6*) have shown that the systems hexane-dodecane, heptane-hexadecane, and hexane-carbon tetrachloride obey this assumption closely. The diffusivities at infinite dilution were computed by the method of King et al. (*13*), which matches the Bidlack and Anderson data well.

Since the liquid-phase diffusivities were strong functions of composition, the computer calculation for k_ϕ was modified to provide for a computation of a value of diffusivity at the concentration corresponding to each point in the Crank-Nicholson matrix. These diffusivities were used in the computation of the next set of concentrations in the iterative procedure.

The solution of the convective diffusion equation for each phase was carried out by using physical properties evaluated at the known value of T_0. This procedure constituted a major simplification, since it eliminated any need to solve the mass and heat transfer problems simultaneously. The assumption was a reasonable one in view of the relative insensitivity of gas-phase properties to temperature and the fact that the penetration of the temperature profile into the liquid was much deeper than that of the concentration profile.

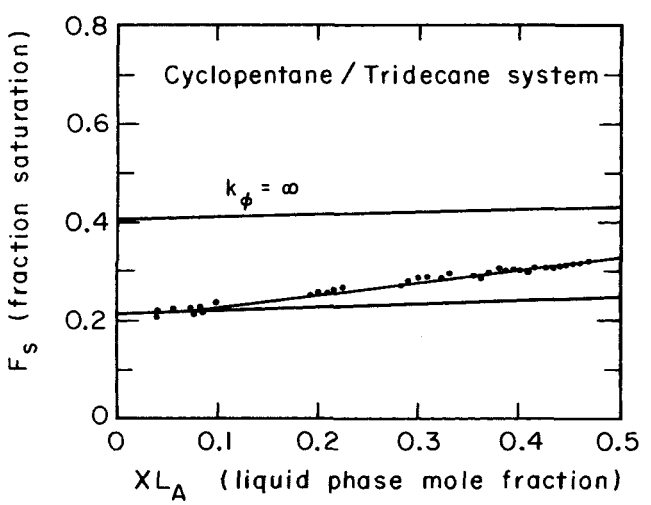

Fig. 3. Evaporation of cyclopentane from *n*-tridecane. $T_0 = 25°C$.

EXPERIMENTAL RESULTS

Figure 1 shows the results for the evaporation of carbon disulfide from *n*-tridecane into nitrogen, plotted as F_s vs. bulk liquid mole fraction of solute. The lower solid line represents the results of the trial-and-error addition of resistances calculation of the interphase mass transfer rate for this system. The upper solid line gives the results for the system if the liquid-phase resistance is hypothetically taken to be negligible compared with the gas-phase resistance. As can be seen, the resistance to mass transfer is nearly evenly divided between phases. The experimental data agree fairly well with the theoretical curve, up to a liquid-phase mole fraction of 0.300. Figures 2, 3, and 4 give a comparison of experimental results with theory on a similar basis for three other solutes evaporating from *n*-tridecane. As can be seen, the agreement for these systems is quite poor, with the ethyl ether system showing the most marked deviation from the predicted behavior. Full experimental data are reported elsewhere (*10*).

The mass transfer behavior of the *n*-pentane, cyclopentane, and ethyl ether systems was traced to a form of cellular convection which was operative in the liquid phase. Under close visual examination of the liquid in the surface region, small streamers could be seen, which were moving in a vertical direction as they were swept along by the fluid motion.

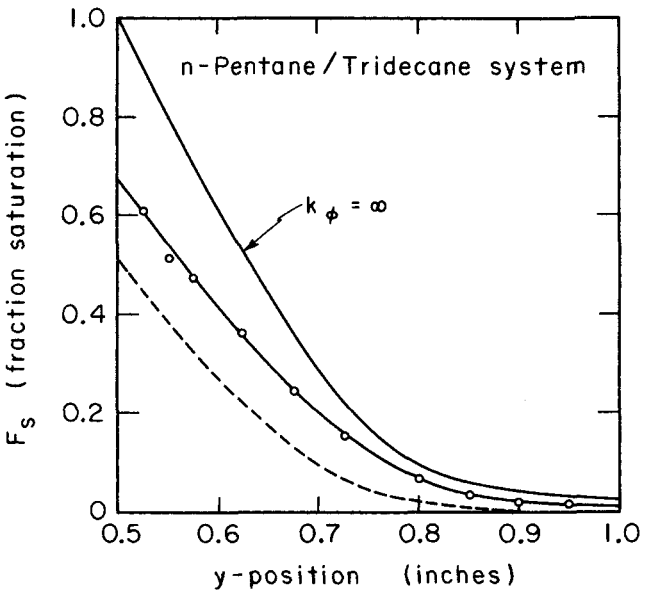

Fig. 5. Gas-phase concentration profile at channel exit for evaporation of *n*-pentane from *n*-tridecane. $XL_A = 0.185$; $T_0 = 20°C$.

A confirmation that the anomalous mass transfer behavior was caused by a liquid-phase phenomenon is given in Figure (5), which represents an experimentally obtained concentration profile for the *n*-pentane system. As can be seen, the experimental profile is at an intermediate position between the predicted profile and the profile for $k_\phi = \infty$, which again indicates that the liquid-phase mass transfer coefficient is much higher than its predicted value, while the gas phase is behaving in the manner predicted. Using the experimental values of x_{A0} and F_s, we can calculate a value of $k_\phi(\text{exp})/k_\phi(\text{theory})$ of 1.4, whereas a calculation of $k_x(\text{exp})/k_x(\text{theory})$ from the same data was found to be 0.921. Thus, the gas-phase coefficient was within 8% of its predicted value, whereas the liquid coefficient was off by 40%. The presence of cellular convection cells in the liquid near the interface should impart some secondary motion to the gas phase through the conservation of momentum across the interface. However, the effect of this motion on gas-phase mass transfer should be much less than the effect upon liquid mass transfer because of the much higher Schmidt numbers in the liquid phase.

Another manifestation of this cellular interfacial motion was a randomly fluctuating output signal from the thermocouple temperature probes (both inlet and outlet) when they were in the liquid phase. The fluctuation was most pronounced in the region 0.025 to 0.10 in. below the liquid surface and probably resulted from the intermittent downward mixing of the cooler interfacial liquid.

After it had been shown that the increased liquid-phase mass transfer coefficient was caused by cellular convection, it was next necessary to ascertain which of four possible mechanisms was producing the flow instability. These four mechanisms can be summarized as:

1. Surface tension driven, induced by temperature gradients.
2. Surface tension driven, induced by concentration gradients.
3. Density driven, induced by temperature gradients.
4. Density driven, induced by concentration gradients.

In order to make this decision, it was necessary to examine the previous work which has been carried out in the area of interfacial cellular convection.

CELLULAR CONVECTION

A large portion of past work on cellular convection has dealt with the onset of instability. The actual driving forces which produce the fluid motion have been shown to be related to the spatial variation of density and surface tension. This variation can be brought about whenever the fluid is undergoing either heat or mass transfer. A listing of the various available mathematical solutions to these stability problems and the assumptions inherent in each can be found in the summary by Berg, Acrivos, and Boudart (5). Temperature induced, density driven cellular motion can occur only if the Rayleigh number

$$N_{Ra} = g\,\beta_T \frac{\partial T}{\partial y} h^4/\alpha\nu \qquad (12)$$

is greater than a given critical value, which ranges from 657 to 1,710, depending upon the applicable boundary conditions for various situations involving linear temperature gradients.

For the temperature induced, surface tension driven phenomenon, cellular convection can occur only if the Thompson number

$$N_{Th} = \left(\frac{\partial \gamma}{\partial T}\right)\left(\frac{\partial T}{\partial y}\right) h^2/\alpha\mu \qquad (13)$$

exceeds 80 for the isothermal case, or 48 for the constant flux case.

Experimental measurements of the onset of cellular convection have, thus far, exhibited a large amount of scatter; however, convection has not been encountered at a Thompson number below the theoretically predicted value. Recent data obtained by Berg (4) give experimentally observed values of critical Thompson numbers which are one to two orders of magnitude higher than the theoretically predicted ones.

An assumption which is inherent in the analyses which have been made of both the density and surface tension driven flows is that of a linear temperature gradient between the upper and lower surfaces. This is often a good assumption for a temperature profile, but for the analogous problems that are caused by concentration gradients it frequently becomes quite poor. This is primarily because of the exceedingly low values of liquid-phase diffusivity, which lead to small penetration depths and therefore nonlinear, undeveloped profiles in many situations. Another difference between the temperature-dependent and the concentration-dependent problems is in the properties entering into the Thompson and Rayleigh numbers; these are given in their concentration-dependent form below:

$$N_{Th} = \left(\frac{\partial \gamma}{\partial C_A}\right)\left(\frac{\partial C_A}{\partial y}\right) h^2/D_{AB}\mu \qquad (14)$$

$$N_{Ra} = g\left(\frac{\partial \rho}{\partial C_A}\right)\left(\frac{\partial C_A}{\partial y}\right) h^4/D_{AB}\nu \qquad (15)$$

Pillow (23) considered the problem of density driven instability in a two-dimensional region between two flat plates at different temperatures. After making several simplifying assumptions, he was able to predict a 5/4 power dependence of heat transfer rate upon the temperature driving force, a number that has been frequently confirmed experimentally for natural convection from a heated horizontal plate (11, 22). Kuo (15) also predicts the 5/4 power dependence, or equivalently the 1/4 power dependence of the Nusselt number upon the Grashof or Rayleigh number for perturbations due to density driven cellular convection. Malkus and Veronis (17) also examined the density driven situation.

There has been relatively little experimental work carried out on the effects of surface tension driven, cellular convection upon mass transfer. Several investigators (*19* to *21*, *26*) have reported increases in liquid-liquid and gas-liquid mass transfer coefficients which they attributed to instabilities of this sort. Bakker et al. (*2*, *3*) used an order of magnitude physical argument to estimate a two to threefold increase in mass transfer coefficients due to interfacial instabilities, which agreed fairly well with their experimental data. Maroudas and Sawistoswki (*18*) have obtained quantitative mass transfer data for liquid-liquid systems undergoing surface tension driven cellular convection. In view of the work which has been carried out thus far, there does not appear to be any satisfactory method for predicting the quantitative effect of surface tension driven cellular convection upon mass transfer coefficients.

EVALUATION OF EXPERIMENTAL RESULTS

Since each of the four mechanisms cited previously can be associated with an appropriate form of the Thompson or Rayleigh group, an estimate of the value of these groups operative during the present experiments should give an indication of which mechanism was most important. A qualitative analysis of the situation shows that any of the above mechanisms could have been responsible for the observed cellular convection in three of the four cases, since all of the driving forces were in the direction leading toward an unstable situation. In order to assign a numerical value to the Thompson and Rayleigh groups, a number of assumptions were necessary because of the large differences between the flow situation at hand and the theoretical problems for which critical Thompson and Rayleigh numbers have been devised.

The concentration and temperature profiles used for obtaining values of h, $\partial C_A/\partial y$, and $\partial T/\partial y$ were calculated by following the simple penetration approach for the liquid phase and by ignoring the presence of the cells. Thus

$$\frac{\partial C_A}{\partial y} = \left(\frac{\partial C_A}{\partial y}\right)_0 = -\Delta C_A \sqrt{\frac{U_{\text{int}}}{\pi D_{AB} x}} \qquad (16)$$

Similarly

$$\frac{\partial T}{\partial y} = \left(\frac{\partial T}{\partial y}\right)_0 = -\Delta T \sqrt{\frac{U_{\text{int}}}{\pi \alpha x}} \qquad (17)$$

h was found from the equations

$$h = \sqrt{\pi D_{AB} x/U_{\text{int}}} \qquad (18)$$

$$h = \sqrt{\pi \alpha x/U_{\text{int}}} \qquad (19)$$

for the concentration dependent and temperature dependent situations, respectively. These equations provide an indication of the depth to which the concentration profile has penetrated, in the absence of convection cells. The recent work of Vidal and Acrivos (*25*) confirms that the definitions made in Equations (16) to (19) are suitable; for these conditions they predict critical Thompson numbers of 4 to 10, if one allows for the fact that their Thompson numbers use b as the length dimension.

All of the other physical properties in the Rayleigh and Thompson groups were assumed to be constant at the values associated with the interfacial conditions. For convenience, the interfacial temperature was taken as the measured value, but the value of interfacial concentration was taken as that obtained by using the interphase solution in the absence of cellular convection. This value is higher than the actual experimental value when cells are present because of the mixing of the liquid phase caused by the existence of any finite cellular convection.

There were several reasons for ignoring the effect of the cellular motion on the interfacial concentration and on the predictions of Equations (16) through (19) for the computation of the Thompson and Rayleigh numbers. First of all, these properties are not altered by cellular motion at or below the critical Rayleigh or Thompson number where the motion first begins. One important reason for neglecting the cell effect above the critical Rayleigh or Thompson number is that one would prefer to determine the influence of the cellular convection from a direct and noniterative calculation based upon known or easily predicted quantities. A second reason is based upon the assumption that the magnitude of the cellular convection effect is a function of the driving force, or the ratio of the Thompson or Rayleigh group to the critical value. If this is a correct assumption, then it is only necessary to employ values of temperature and concentration gradients, h, and interfacial concentration uniquely related to the true value. The proposed method is a convenient approach for obtaining such a value.

Upon calculation of the Thompson or Rayleigh numbers for each of the four possible situations, it was discovered that the surface tension driven, concentration gradient induced mechanism yielded a value of the Thompson number which was two orders of magnitude larger in relation to the critical N_{Th} or N_{Ra} than occurred for the other mechanisms. To illustrate the values of N_{Th} and N_{Ra} in the four situations, the results of a sample calculation carried out for n-pentane/tridecane at a pentane mole fraction of 0.05 are: for the concentration gradient induced case $N_{Th} = 13{,}900$ and $N_{Ra} = 26$; for the temperature gradient induced case $N_{Th} = 93$, and $N_{Ra} = 155$. These values of the Rayleigh and Thompson groups are averaged along the entire channel length; since N_{Ra} and N_{Th} vary as $x^{1/2}$, the average is two-thirds of the value at the exit probe.

Of the four mechanisms, two tend to predominate, the concentration gradient induced, surface tension driven instability and the temperature gradient induced, density driven instability. This is primarily due to the dependence of the groups on h, which is h^2 for N_{Th} and h^4 for N_{Ra}. Because of the extremely low value of the liquid-phase diffusivities, h tends to be quite small for the concentration profile; thus the value of N_{Th} tends to be much larger than the value of N_{Ra} for the concentration dependent situation. For the temperature dependent forms, the reverse is true. The penetration depths for the temperature profiles tend to be fairly large, making the density driven situation relatively more important than the surface tension driven one.

The carbon disulfide/n-tridecane system should not exhibit concentration gradient induced cellular convection, since both the density and the surface tension of carbon disulfide lie in the wrong direction from that of tridecane. The results for this system shown in Figure 1 support this conclusion, with the agreement between experiment and interphase theory remaining quite good at values of XL_A up to 0.30 or more. This good agreement for the carbon disulfide system serves to substantiate the validity of the approach used for the prediction of interphase mass transfer rates in the absence of cellular convection.

The deviation which finally begins to occur in the carbon disulfide/tridecane data at the higher concentration levels can be attributed to temperature gradient induced, density driven cells. This hypothesis is supported by the calculated value of the Rayleigh number for the carbon

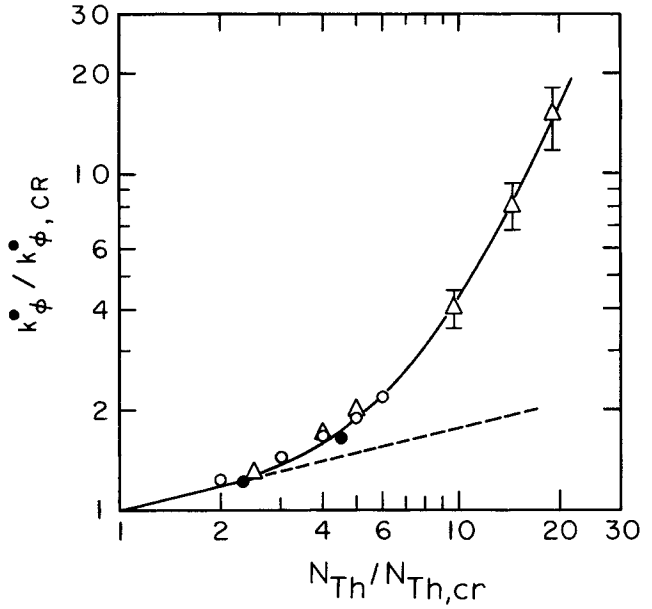

Fig. 6. Correlation of the effect of surface tension driven cellular convection upon liquid-phase mass transfer coefficients.

△—ethyl ether/tridecane system

○—*n*-pentane/tridecane system

●—cyclopentane/tridecane system

disulfide/tridecane system at $XL_A = 0.30$. N_{Ra} is 1,600, a value which is significantly larger than the theoretical critical value of approximately 650. To show that the cellular convection in the three other experimental systems was apparently not strongly influenced by density driven cells, the values of XL_A which yield a calculated value of $N_{Ra} = 1{,}600$ are $XL_A = 0.24$ for *n*-pentane/tridecane, $XL_A = 0.27$ for cyclopentane/tridecane, and $XL_A = 0.22$ for ethyl ether/tridecane.

Convection cells in the liquid near the interface were also noticed for the evaporation of pure liquids discussed in part I. This occurred at high liquid volatilities and resulted in a noticeable lessening of the interfacial temperature depression. Presumably these cells resulted from the temperature gradient induced, density driven mechanism.

Since the majority of the cellular convection appeared to be attributable to the concentration gradient induced, surface tension driven mechanism, an effort was made to correlate the mass transfer behavior of the liquid phase with the physical parameters which lead to this type of cellular convection. It was found that a single value of $N_{Th,cr} = 8{,}000$ was sufficient to predict the point of instability of all the experimental systems studied. The values of XL_A which correspond to $N_{Th,cr} = 8{,}000$ are given below:

n-pentane/tridecane	$XL_{A,cr} = 0.029$
ethyl ether/tridecane	$XL_{A,cr} = 0.014$
cyclopentane/tridecane	$XL_{A,cr} = 0.071$

The Thompson numbers at which cellular convection first has an appreciable effect on the mass transfer coefficient are thus several orders of magnitudes above the critical values which have been predicted by stability theory.

Dimensional analysis of the mass transfer situation leads to the following expressions:

$$N_{Sh} = f(N_{Th}, N_{Sc}, N_{Re}) \text{ above } N_{Th,cr} \qquad (20)$$

and

$$N_{Sh} = f'(N_{Sc}, N_{Re}) \text{ at or below } N_{Th,cr} \qquad (21)$$

From the above two expressions, and in view of the results obtained by Kuo (*15*) and others for the somewhat analogous heat transfer problem, it appears that a reasonable form for correlation of the experimental data is

$$\dot{k}_\phi / \dot{k}_{\phi,CD} = f\left[\frac{N_{Th}}{N_{Th,cr}}, N_{Sc}, N_{Re}\right] \qquad (22)$$

The variable $\dot{k}_{\phi,CD}$ is the value of the liquid-phase mass transfer coefficient which is predicted theoretically by simple convective diffusion theory, the value at or below the point where the flow instability is first observed, with concentration, flux and physical property corrections to the actual concentration level taken into account.

A correlation of the type given by Equation (22) has the advantage of giving the increase in mass transfer due to cellular convection effect alone. Thus, the resistance to mass transfer in the presence of cellular convection is obtained by simply multiplying the expected liquid-phase mass transfer coefficient by a correction factor to obtain the actual mass transfer coefficient.

The experimental results of this study are shown in Figure 6, plotted in the form suggested by Equation (22). As can be seen, the agreement between the three different systems, *n*-pentane, cyclopentane, and ethyl ether, is quite good when placed on this basis. It is interesting to note that the increase in the mass transfer coefficient due to cellular convection can be quite large for some systems, such as the ethyl ether/tridecane mixture where the observed value of $\dot{k}_{\phi,avg}$ reached ten to twenty times the expected value. Another fact which may be observed from Figure 6 is that the initial slope is approximately the same as indicated by the nonlinear heat transfer analysis for density driven cells, a one-quarter power dependence upon the Thompson (or Rayleigh) number ratio (*15, 23*). The dashed straight line in Figure 6 indicates the one-quarter power dependence and can be seen to be tangent to the results obtained experimentally in the vicinity of the critical value of the Thompson number.

An examination of the quantities entering into the correlation given by Figure 6 shows that the correlation is essentially one of $\dot{k}_\phi/\dot{k}_{\phi,cr}$ vs. $\Delta\varphi/\Delta\varphi_{cr}$, since the other quantities in the Thompson number are only weak functions of concentration. There are several other factors which need to be explored in more detail experimentally and theoretically. Among these are the effect of the ratio of gas- to liquid-phase mass transfer coefficient, k_x/k_ϕ, which was varied only slightly during this work. Substantial changes in this ratio could invalidate the procedure used to calculate $\varphi_{A\infty} - \varphi_{A0}$ for use in the Thompson number. A second point is that the liquid depths utilized in this study were rather large; therefore, any application of these results to systems having very small liquid depths, or differing flow characteristics, should be made with caution. Because of the similar physical constants of the liquid systems involved, the Schmidt number variation was not large, and therefore the effect of Schmidt number, if any, could not be determined. Also, the effect of different liquid-phase Reynolds numbers was not explored in this work. Further experimental work with more diverse systems at widely different flow rates should be carried out to define the effects of these two groups. Finally, minute concentrations of surface-active impurities could radically affect the flow characteristics of the surface tension driven cellular convection. This type of situation would be most likely to occur in an aqueous system, usually bringing about a large reduction in the amount of cellular convection from that which would be predicted for such a system.

CONCLUSIONS

Part I

1. A high flux solution has been obtained for the case of a linear velocity gradient in a semi-infinite flowing fluid (the Leveque model).

2. The high flux and high concentration level correction factors proposed in this work have been confirmed experimentally for the case of evaporation of pure volatile liquids into a flowing gas stream.

3. A simple calculational approach has been developed for the prediction of the effect of mass transfer upon the interfacial temperature of a liquid (or liquid mixture) evaporating into a laminar gas stream. This method was confirmed experimentally.

Part II

4. A trial-and-error addition of resistances technique has been developed to predict interphase, high flux, and high concentration level mass transfer rates. This procedure was also confirmed experimentally for the evaporation of carbon disulfide from *n*-tridecane into nitrogen.

5. An experimental correlation has been developed which accurately predicts the effect of surface tension driven cellular convection upon the average liquid-phase mass transfer coefficient, provided the Reynolds number and Schmidt number variations are not large.

ACKNOWLEDGMENT

This work was performed in the Lawrence Radiation Laboratory under the auspices of the U.S. Atomic Energy Commission.

NOTATION

c = total concentration, g.moles/cc.
C_A = concentration of species A, g.moles/cc.
D_{AB} = diffusion coefficient in the binary system A-B, sq.cm./sec.
g = acceleration due to gravity, cm./sq.sec.
H = Henry's law constant, atm.cc./g.moles
h = depth of a liquid layer, cm.; also used in this study as the penetration depth of a concentration or temperature profile in the liquid phase
k = mass transfer coefficient at low flux conditions, g.moles/sq.cm.sec.
$\overset{\bullet}{k}$ = mass transfer coefficient (applicable at high flux conditions), g.moles/sq.cm.sec.
N_A = molar flux of component A relative to stationary coordinates, g.-moles/sq.cm.sec.
N_{Gr} = Grashof number, dimensionless
N_{Pr} = Prandtl number, dimensionless
N_{Nu} = Nusselt number, dimensionless
N_{Ra} = Rayleigh number, dimensionless
N_{Re} = Reynolds number, dimensionless
N_{Sc} = Schmidt number, dimensionless
N_{Sh} = Sherwood number, dimensionless
N_{Th} = Thompson number, dimensionless
P = pressure, atm.
R_{AB} = dimensionless flux ratio
T = temperature, °C.
$\tilde{V}$ = partial molal volume, cc./g.mole
x = horizontal distance variable, cm.
x_A = mole fraction of component A (used in gas phase)
XL_A = liquid-phase mole fraction of component A (volatile solute)
y = vertical distance variable, cm.

Greek Letters

α = thermal diffusivity, sq.cm./sec.
β = coefficient of thermal expansion, $°C^{-1}$
γ = surface tension, dynes/cm.
Δ = difference in quantity between interfacial and bulk conditions
θ_{AB} = dimensionless flux correction factor
μ = viscosity, poises
ν = kinematic viscosity, stokes
φ_A = volume fraction of component A (used in liquid phase)

Variable Subscripts

A, B = components A, B, etc.
AB = the binary system composed of components A and B
avg. = average of a quantity
CD = predicted by simple convection diffusion theory
cr = at the critical point for cellular flow instability
G = gas
L = liquid
loc = local or point value
0 = quantity evaluated at the interfacial position
x = based upon mole fractions (used for gas phase)
φ = based upon volume fraction (used for liquid phase)
∞ = quantity evaluated at a large distance from the gas-liquid interface, equivalent to inlet conditions

LITERATURE CITED

1. American Chemical Society, *Adv. Chem., No. 22,* **2,** (1959).
2. Bakker, C. A. P., P. M. Buytenen, and W. J. Beek, *Chem. Eng. Sci.*, **21,** 1039 (1966).
3. ———, F. H. Fentener van Vlissingen, and W. J. Beek, *ibid.*, **22,** 1349 (1967).
4. Berg, J. C., Ph.D. thesis, Univ. California, Berkeley (1964).
5. ———, A. Acrivos, and M. Boudart, "Advances in Chemical Engineering," Vol. 6, Academic Press, New York (1966).
6. Bidlack, D. L., and D. K. Anderson, *J. Phys. Chem.*, **68,** 3790 (1964).
7. Byers, C. H., and C. J. King, *U. S. Atomic Energy Comm. Rept* UCRL-16535 (1966).
8. ———, *AIChE J.*, **13,** 628 (1967).
9. *Ibid.*, 637.
10. Clark, M. W., and C. J. King, *U. S. Atomic Energy Comm. Rept.* UCRL-17527 (1967).
11. Jakob, M., "Heat Transfer," Vol. 1, John Wiley, New York, (1949).
12. King, C. J., *AIChE J.*, **10,** 671 (1964).
13. ———, L. Hsueh, and K. Mao, *J. Chem. Eng. Data,* **10,** 348 (1965).
14. Koefoed, J., and J. V. Villadsen, *Acta Chem. Scand.*, **12,** 1124 (1958).
15. Kuo, H. L., *J. Fluid Mech.*, **10,** 611 (1961).
16. Lewis, W. K., *Mech. Eng.*, **44,** 445 (1922).
17. Malkus, W. V. R., and G. Veronis, *J. Fluid Mech.*, **4,** 225 (1958).
18. Maroudas, N. G., and H. Sawistowski, *Chem. Eng. Sci.*, **19,** 919 (1964).
19. Merson, R. L., and J. A. Quinn, *AIChE J.*, **11,** 391 (1965).
20. *Ibid.*, **10,** 804 (1964).
21. Muenz, K., and J. M. Marchello, *ibid.*, **12,** 249 (1966).
22. Perry, R. H., "Chemical Engineers Handbook," 4th ed., McGraw-Hill, New York (1963).
23. Pillow, A. F., *Aeronaut. Res. Rept. Australia,* **A79,** 1 (1952).
24. Timmermans, J., "Physico-chemical Constants of Pure Organic Compounds," Elsevier, New York (1950).
25. Vidal, A., and A. Acrivos, *Ind. Eng. Chem. Fundamentals,* **7,** 53 (1968).
26. Ward, W. K., and J. A. Quinn, *AIChE J.*, **11,** 1005 (1965).
27. Whitman, W. G., *Chem. Met. Eng.*, **29,** 146 (1923).

Manuscript received December 5, 1967; revision received June 7, 1968; paper accepted June 12, 1968.